SPRINGER LINK

Log in

Menu Search Cart

Home Journal of Nanoparticle Research Article

Contribution in PCE enhancement: numerical designing and optimization of SnS thin film solar cell

Research paper Published: 12 July 2021

Volume 23, article number 146, (2021) Cite this article

Download PDF

Access provided by Dr. Babasaheb Ambedkar Marathwada University, Aurangabad

Journal of Nanoparticle Research

Aims and scope

Submit manuscript

Vishnu V. Kutwade, Ketan P. Gattu, Makrand E. Sonawane, Dipak A. Tonpe, Manoj K. Mishra & Ramphal Sharma

541 Accesses 11 Citations Explore all metrics →

Abstract

This study aims to improve the experimentally low performance of p-SnS/n-ZnMgO thin film solar cells (TFSCs). We report a modification in the p-SnS/n-ZnMgO cell structure to address the issues with the help of detailed numerical modeling and analysis via solar cell capacitance simulator software (SCAPS). Here, CdS is used as a thin buffer layer about a few nanometers in between the p-SnS absorber layer and n-ZnMgO window layer. However, in terms of band alignment, SnS/CdS interface attributed the minimum band-offset, resulting in the enhancement of open-circuit voltage (V_{oc}) and overall performance. Furthermore, to evaluate the final cell structure, the solar cell simulation has been investigated by varying several parameters such as thickness and defect density of absorber layer; interface defect density and the operating temperature affect the electrical parameters of TFSCs.

Initially, the band-alignment engineering has been investigated for variable doping concentration (x) of magnesium (Mg) in the $Zn_{1-x}Mg_xO$ window layer. However, Mg concentration (x) = 0.18 shows the better results (Voc = ~ 0.7 V, short-circuit current density (Jsc) = 38.54 mA/cm^2, Fill Factor = 83%, and efficiency (η) = ~ 23%) with minimum band-offset at the CdS/ZnMgO interface, and the hexagonal nanorod-like morphology of ZnMgO helps to improve open-circuit voltage. Finally, with the optimized parameters (t_{SnS} = 2 μm, t_{CdS} = 50 nm, and t_{ZnMgO} = 70 nm) with maximum SnS/CdS interface defect density ($N_t = 1 \times 10^{11}$ cm^{-2}), the simulated optimal p-SnS/CdS/n-ZnMgO cell structure exhibited the highest efficiency ~ 20% comparably higher than the reported p-SnS/n-ZnMgO experimental value of 2.1%.

Similar content being viewed by others

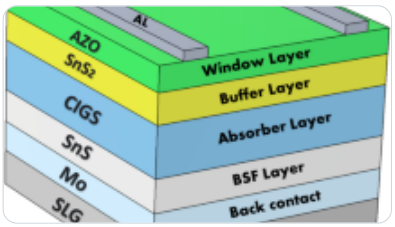

Efficiency Enhancement by BSF Optimization on Cu (In1-x, Gax) Se2 Solar Cells with Tin (IV) Sulfide Buffer...

Article | 18 April 2023

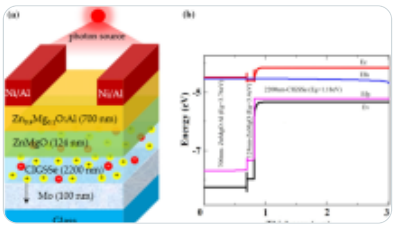

Performance Enhancement of ZnMgO:Al/ZnMgO/ CIGSSe Solar Cell With the Combination of CZTGSe HT...

Article | 15 September 2021

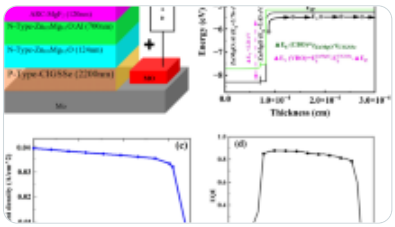

The impact of SnMnO2 TCO and Cu2O as a hole transport layer on CIGSSe solar cell performance improvement

Article | 14 June 2023

Use our pre-submission checklist →

Avoid common mistakes on your manuscript.

Introduction

A thin-film solar cell (TFSCs) in the photovoltaic industry provides a very clean, cost-effective, trustworthy, and perpetual means for meeting the ever-increasing global sustainable and renewable energy demand. Among the many chalcogenide compounds, IV–VI group tin sulfide (SnS) semiconductor has been known to contribute to the PV industry and its development has been studied by different research groups (Devika 2008; Ghosh 2011; Sinsermsuksakul et al. 2014; Ramakrishna Reddy et al. 2006; Minbashi 2018; Baig 2018). Researchers have found that SnS resembles high-cost absorber materials and can be made a paramount absorber layer for TFSCs due to its intrinsic

properties such as high optical absorption coefficient ($\alpha \sim 10^5$); direct bandgap energy of 1.1–1.3 eV; high free carrier concentration ~ 10^{12}–10^{18} cm^{-1}, along with high external quantum efficiency (EQE); a long minority carrier diffusion length; and a low recombination velocity. Furthermore, SnS (Herzenbergite) consist of earth-abundant, non-toxic materials, and it is stable in both acidic/alkaline conditions. The theoretical limit of efficiency for SnS with a bandgap of 1.1 to 1.3 eV is around 32% under an AM 1.5 G solar spectrums at 1000 W/m^2 (Ramakrishna Reddy et al. 2006; Andrade-Arvizu et al. 2015; Rühle 2016). The numerical analysis for SnS-based TFSCs has also been studied to enhance its PV properties (Ghosh 2011; Klochko 2016; Xu and Yang 2014; Haleem and Ichimura 2010). Mg-doped ZnO (ZnMgO), an earth-abundant and non-toxic material, was explored both as a buffer layer as well as a window layer for SnS, CIGS, and CdTe-based TFSCs. The electrical and optical parameters of ZnMgO material have been well explored with numerical analysis (Maity and Sahu 2019; He 2019; Chantana et al. 2019; Bittau 2018). For SnS-based TFSCs, ZnMgO as a window layer could be considered a potential candidate. ZnMgO has a tunable wide-bandgap from 3.2 to 3.8 eV controlled with varying concentrations of magnesium; this helps to improve short-circuit current density. In addition to this, ZnMgO provides a band alignment and electron affinity suitable for SnS-based solar cells. The electron affinity decreases with the increase in the bandgap; this shift in electron affinity leads to the creation of sufficient distribution of heterojunction electric fields and it keeps photo-generated carrier recombination from happening. To achieve better PCE SnS-based solar cells, we need to study in detail and explore more using the buffer layer between SnS/ZnMgO interfaces. Furthermore, a thin CdS buffer layer perfectly fits between these two materials according to energy band alignment and stabilizes the cell structure by minimizing the difference between the conduction band (Cho 2019; Hertwig et al. 2020). This investigation could help in the development of SnS-based TFSCs. Although several types of software offer numerical investigations using simulations to explore the effect of physical parameters and to measure the optimum photovoltaic parameters, here, we used SCAPS-1D software for numerical analysis of the proposed SnS-based TFSCs. SCAPS-1D software with graphical user interface (GUI) was primarily developed to simulate CIGS and CdTe TFSCs by Marc Burgelman et al. (Burgelman et al. 2007) and is widely used for numerical analysis, simulation, and development of 1D TFSCs.

In this paper, SCAPS-1D software has been used to explore SnS-based TFSCs using $Zn_{1-x}Mg_xO$ as a window layer and CdS as a buffer layer. This study aims to overcome the failure of agreement between predicted Shockley-Queisser theoretical and the reported experimental values of efficiency of SnS/ZnMgO solar cell structure. From this standpoint, considering the band alignment factor, the CdS buffer layer has been introduced in the proposed cell structure and also analyzed the effect of different Mg concentrations on the proposed cell structure. Several different semiconductor parameters play a vital role in the fabrication of TFSCs. We analyze in detail the performance of TFSCs with the help of semiconductor equations by variation in parameters such as the absorber layer thickness and defect

density, SnS/CdS interface defect density, concentrations (x) of Mg in $Zn_{1-x}Mg_xO$ window layer, and also the band alignment between absorber/buffer/window layers to obtain the highest achievable PCE.

Modeling

Cell structure and material parameters

According to the detailed literature survey and the best of the author's knowledge, no one has explored simulation of p-SnS/CdS/n-ZnMgO heterojunction for thin film solar cell application using SCAPS. Marc Burgelman et al. have developed a program for thin film solar cells in a way that it is possible to program simulation for seven-layered cell structure excluding front and back contact layers (Burgelman et al. 2007). Figure 1 shows the proposed SnS-based TFSCs design which consists of three layers for simulation.

- Absorber layer:- p-SnS with a bandgap of 1.2 eV and thickness 2 μm
- Buffer layer:- n-CdS with a bandgap of 2.4 eV
- Window layer:-n-ZnMgO wide-bandgap transparent oxide semiconductor

Fig. 1

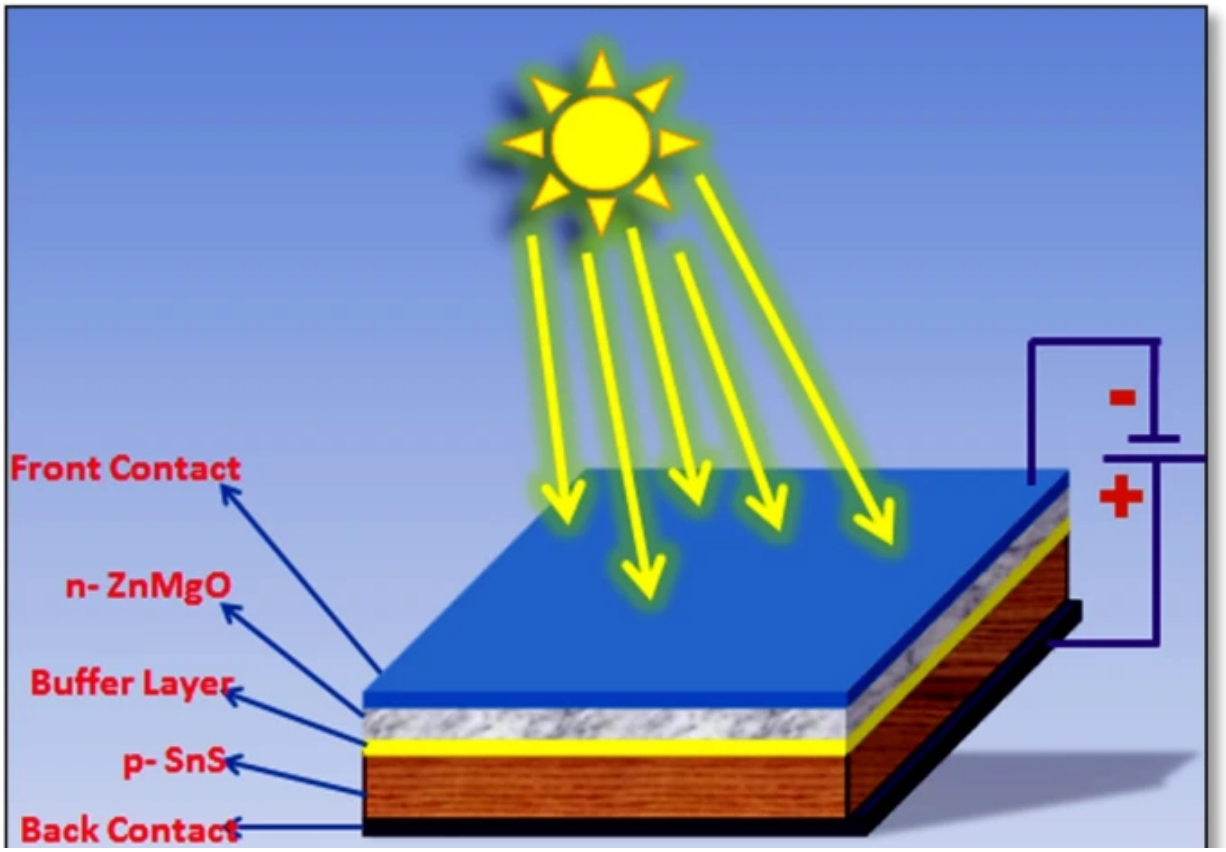

Schematic diagram of the proposed solar cell structure

A thin layer of CdS lies in between the sandwich of SnS absorber layer and ZnMgO window layer, resulting in the enhancement of the performance of SnS/ZnMgO thin film solar cell. Front contact which is below the window layer (ZnMgO) where AM 1.5 global spectrums with a light power of 1000 W/m^2 are used to incident light. Both front and back contact properties are also accounted for solar cell simulation. Here, in the present simulation, for both the contacts, the flat band has been chosen. The required optical and electrical parameters of SnS, CdS, and ZnMgO layer materials are collected from reported literature. These optimized material parameters are used as input values for numerical analysis, solving the semiconductor equations such as the Poisson equation and continuity equation using the SCAPS-1D simulation program. Table 1 representing the device input parameters used in the simulation.

Table 1 Input parameter details used for simulation of SnS-based solar cell

Result and discussion

Band diagram

The band configuration is one of the most essential aspects which affect the transportation of photo-generated carriers through the interfaces, carrier recombination, and overall execution of the solar cells. For SnS-based TFSC, p-SnS/CdS/n-ZnMgO band-edge model using SCAPS-1D simulation under luminous condition is shown in Fig. 2. The proposed heterojunction TFSC structure under the light illumination generates carriers that result in Fermi-level splitting into quasi-Fermi levels (E_{fn} and E_{fp}) (Tebyetekerwa 2019). These quasi-Fermi levels are responsible for the open-circuit voltage (V_{oc}) of the device. As seen in Fig. 2, the interface between SnS/CdS (Xu and Yang 2014) and CdS/ZnMgO (Andrade-Arvizu et al. 2015) both show type II heterojunction. Although few other buffer layers are available which can be placed in between the SnS/ZnMgO (Reddy et al. 2011), here in the present case, CdS has been introduced in terms of band alignment and other factors like lattice mismatch between SnS/CdS interface. In terms of band-edge positions, conduction band edge (E_C) = − 4.05 eV and valence band edge (E_V) = − 6.45 eV values of CdS lies in between SnS (E_C = − 3.9 eV and E_V = − 5.1 eV) and ZnMgO (E_C =

− 4.5 eV and E_V = − 7.5 eV) layer. This type of heterojunction allows for easy transportation of free-electron between the interfaces of materials.

Fig. 2

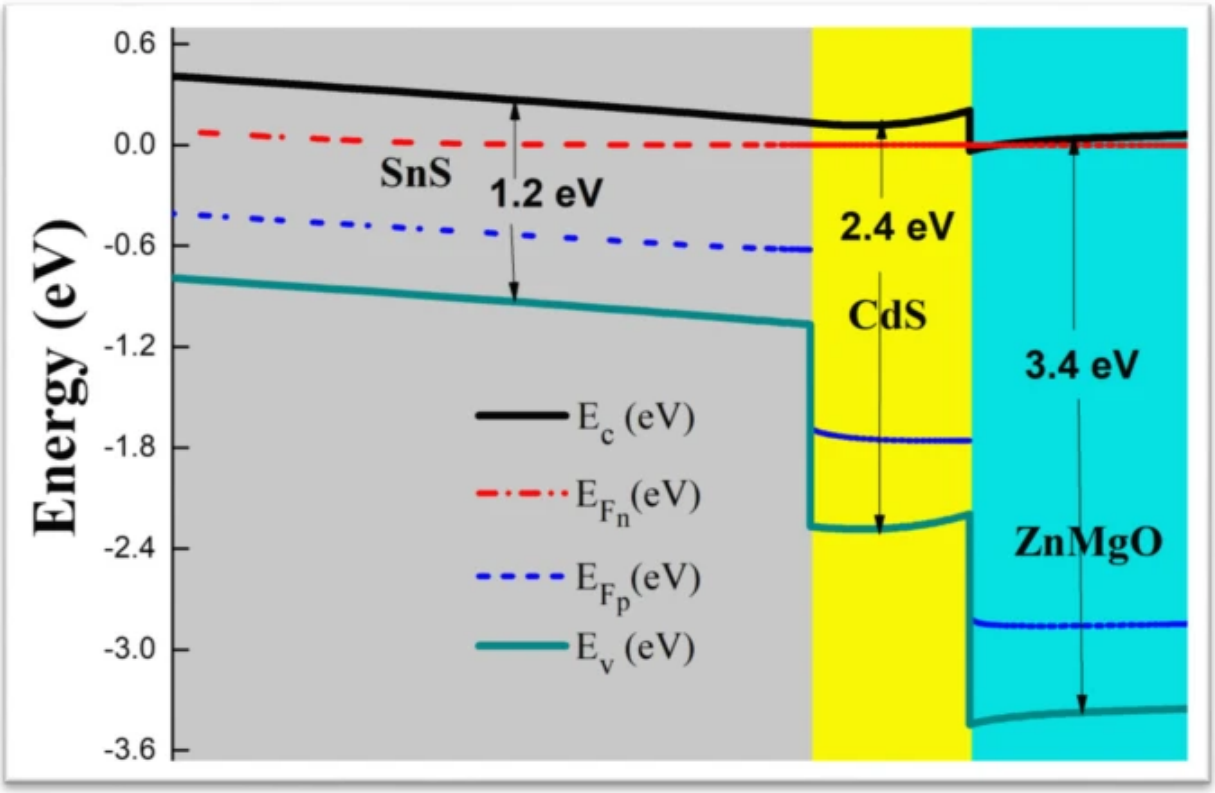

Band-edge diagram of SnS-based solar cell

Furthermore, the factors like thickness and donor/acceptor density of absorber, buffer, and doping concentration in window layer also influence the efficiency of TFSCs and thus are varied in this study.

Effect of composition

To study the impact of compositional change in the ZnMgO window layer, parameters for absorber and buffer layers were kept constant. As the quantity of magnesium increases the bandgap of ZnMgO increases, therefore, J_{SC} is enhanced slightly with the increase of bandgap of the window layer (Gharibshahian et al. 2018; Rajpal and Kumar 2019). Figure 3 shows the dependent relation curve between bandgap and electron affinity with the change in variations of concentration x of Mg in $Zn_{1-x}Mg_xO$. Figure 4 shows the result for change in the band alignment at the interface of SnS/CdS/$Zn_{1-x}Mg_xO$ concerning concentration (x) of Mg, and these results were carried out through the SCAPS simulation program. From the band-edge diagram, we can observe that the band alignment between

the interfaces of SnS/CdS is of type II heterojunction. However, for SnS and CdS, the values of χ are the same 4.2 eV, and from simulation, the conduction band-offset is nearly 0 eV (may be due to the Fermi-level positions and band bending) which is in favor of SnS solar cell performance (Niemegeers et al. 1995).

Fig. 3

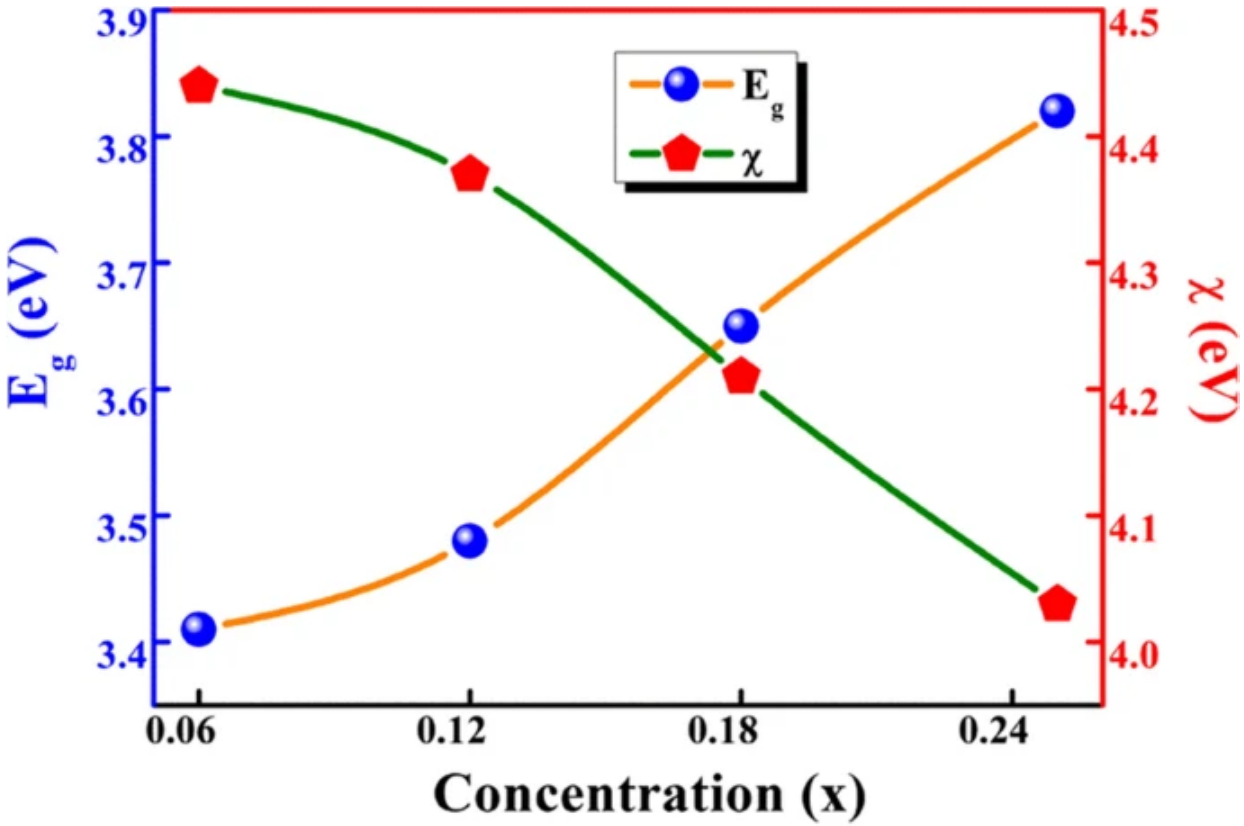

Concentration (x)-dependent bandgap and electron affinity of ZnMgO (He 2018)

Fig. 4

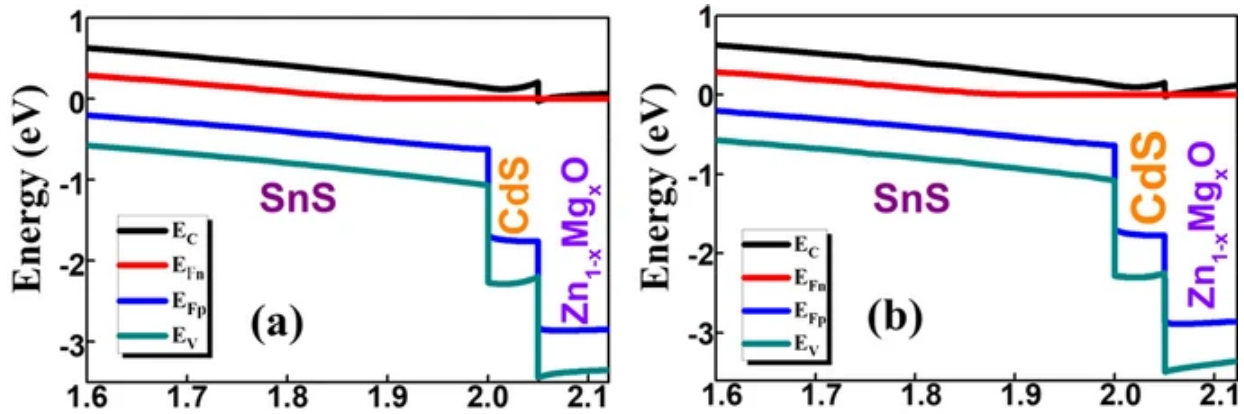

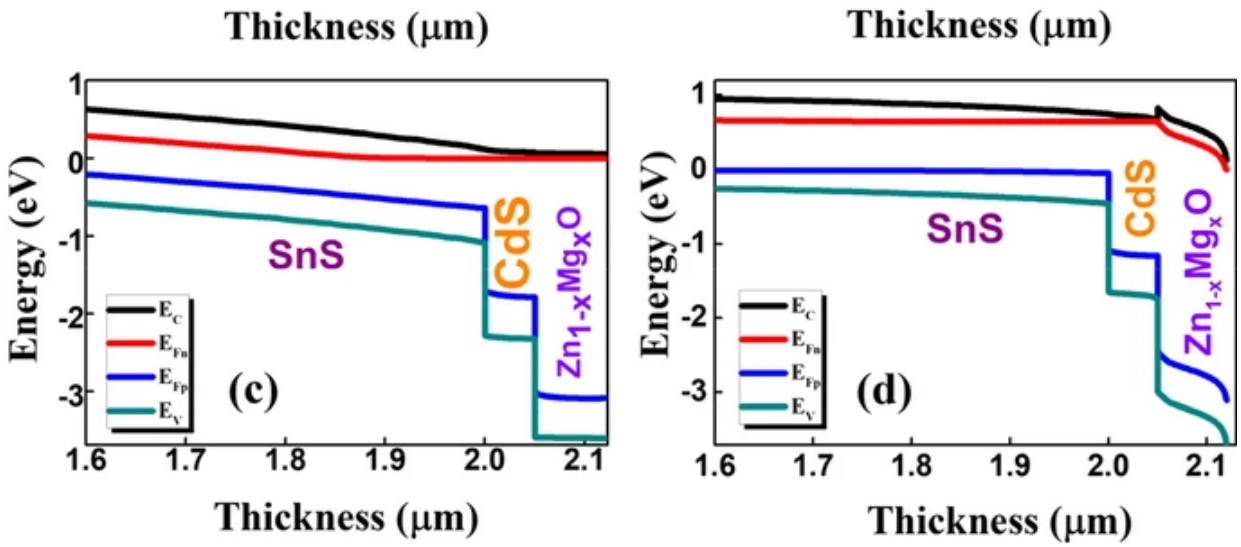

Band alignment diagram for SnS/CdS/$Zn_{1-x}Mg_xO$ TFSCs with Mg concentration **a** x = 0.06, **b** x = 0.12, **c** x = 0.18, and **d** x = 0.25

Figure 4a and b are the band diagrams for SnS/CdS/$Zn_{1-x}Mg_xO$ with Mg concentration x = 0.06 and x = 0.12. Furthermore, at the interface of CdS/$Zn_{1-x}Mg_xO$, the band alignment shows conduction band-offsets (cliff-like structure) and which might be responsible for electron recombination. For concentration x = 0.25, there is a positive conduction band-offset (spikes) at the interface of CdS/$Zn_{1-x}Mg_xO$, as shown in Fig. 4d. This spike-like structure contributes a barrier-like structure which reduces interface recombination. In Fig. 4c the band-offset of nearly 0 eV is in favor of the CdS/ZnMgO interface. Figure 5 shows the change in PV parameters with the concentration x of Mg in $Z_{1-x}Mg_xO$. The band-offset plays an important role in the measurement of PV parameters of SnS solar cells with a concentration of Mg in the $Z_{1-x}Mg_xO$ window layer. As we can see in Fig. 5, for all values of concentration, V_{OC} remains constant at 0.7213 V while current J_{SC} values show variations. J_{SC} values increase with an increase in the concentration of Mg up to x = 0.18, and due to a large spike for x = 0.25, as shown in Fig. 4d, the J_{SC} gradually decreases. Furthermore, the values of FF and efficiencies follow a similar trend. Both values are nearly the same for the concentration x = 0.06 to 0.18 and then suddenly decreases for x = 0.25 (Mohammadnejad et al. 2020).

Fig. 5

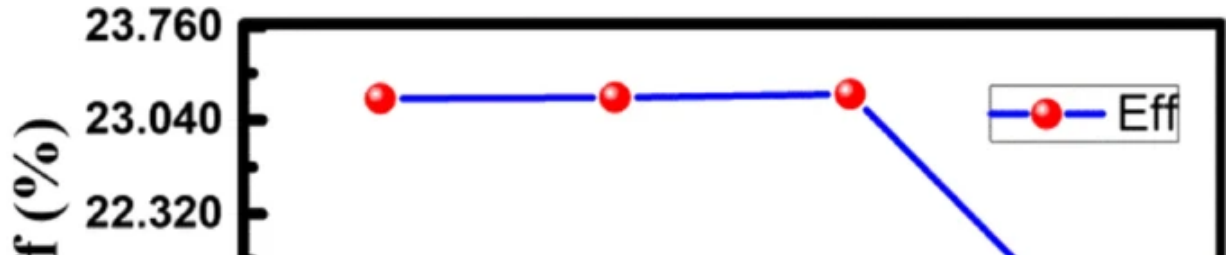

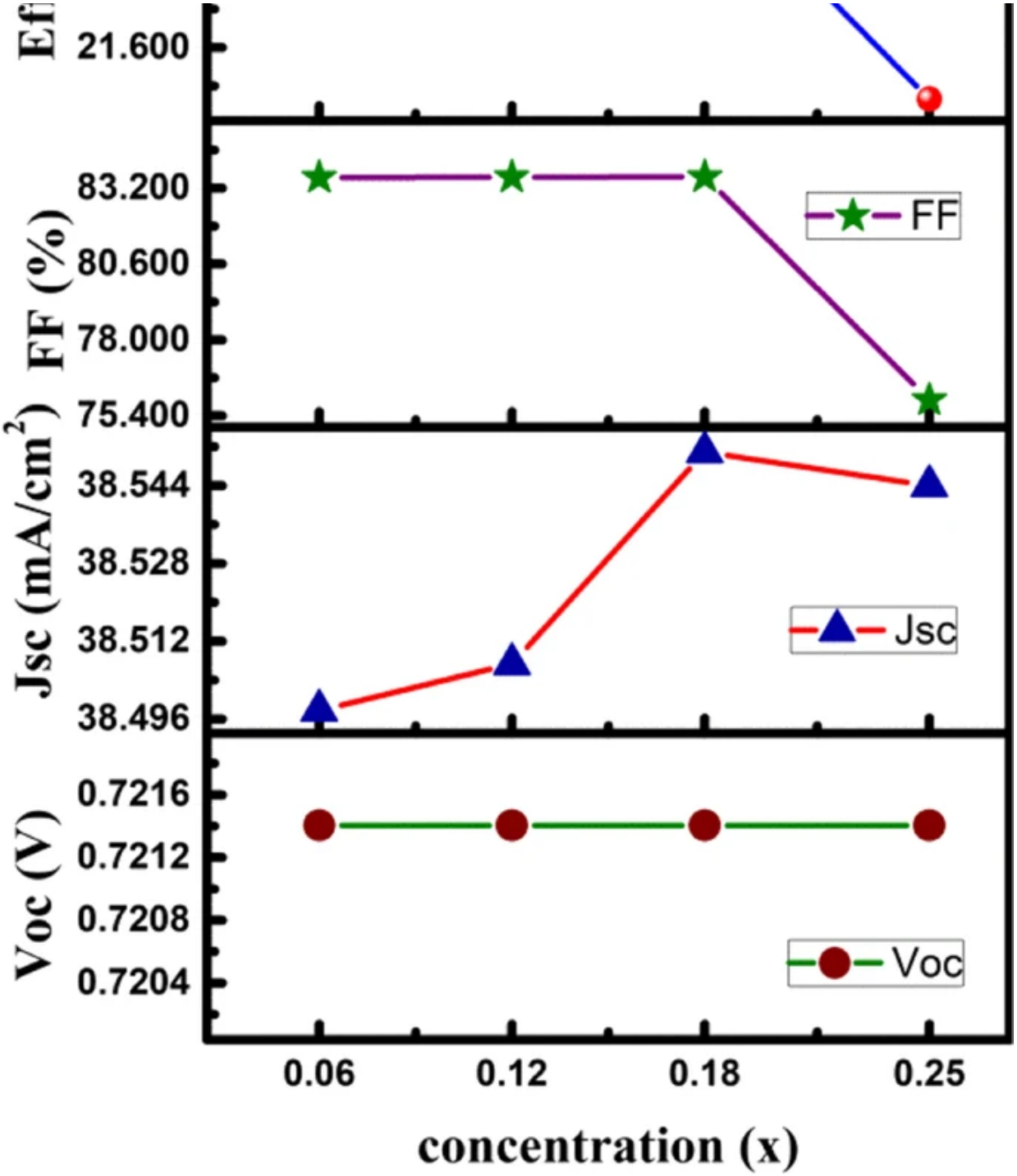

Effect of concentration (x) of Mg on the performance of the solar cell

Effect of SnS absorber layer thickness

In the above simulations, we have chosen the optimized thickness of 2 μm for the SnS absorber layer from reported literature (Baig 2018; Garain et al. 2021). The thickness of the absorber layer influences solar cell performance; with the variation of thickness, the resulted solar cell parameters are shown in Fig. 6. The results show that the solar cell performance significantly decreased below 2 μm, while for

thickness above 2 μm, there was no significant change. Thus, 2 μm was chosen as the optimized thickness as a further increase in thickness would increase the unwanted defects.

Fig. 6

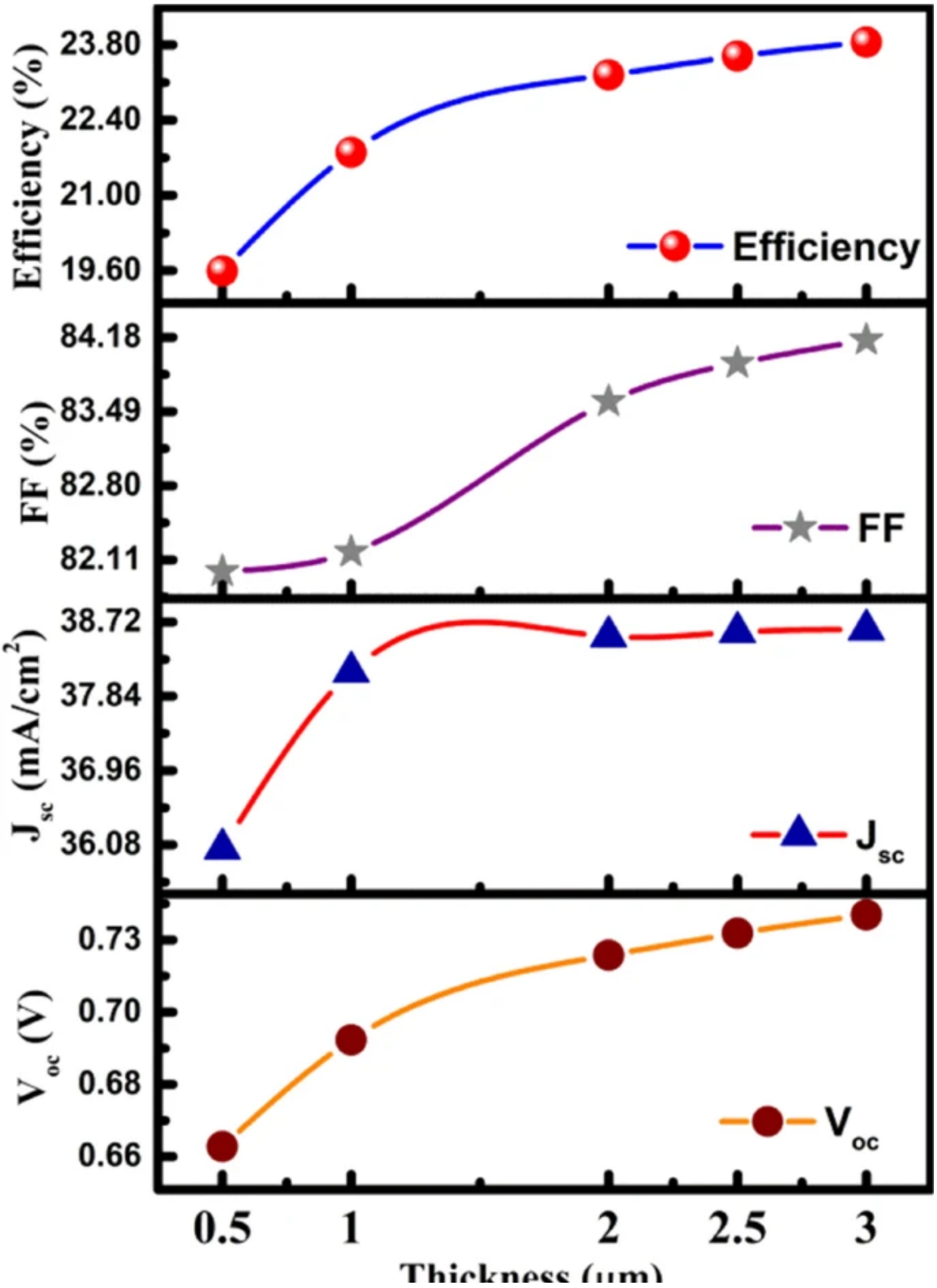

Thickness (μm)

Solar cell performance with the thickness of the absorber layer

Influence of defect density on the performance of solar cell

Since we know that the performance of SnS-based solar cells is largely dependent on several factors, these factors are affected by defect parameters. In this section, the impact of defect parameter investigation was studied for the absorber layer and the interface of SnS/CdS layers, which mostly affect the performance of the solar cell. The defect parameters are tabulated in Table 2.

Table 2 Defect parameters for cell structure

Absorber layer

Here the defect density parameter is introduced in the absorber layer; the values are depicted as in Table 2. The performance of the solar cell was investigated with the change in defect density (N_t). The output results of the solar cell are shown in Fig. 7; we can see the increase in defect density degraded the performance. The efficiency is approximately constant until $N_t = 1 \times 10^{10}$ cm^{-3}, with further increase in the defect density, the efficiency decreases up to nearly 20%. For defect density value $N_t = 1 \times 10^{14}$ cm^{-3}, the efficiency of solar cells significantly decreases to $\eta = 20.19\%$ which is ~ 4% less than the optimized efficiency value. The defects in the absorber layer increase the bulk recombination probability, and the performance of solar cells degrades.

Fig. 7

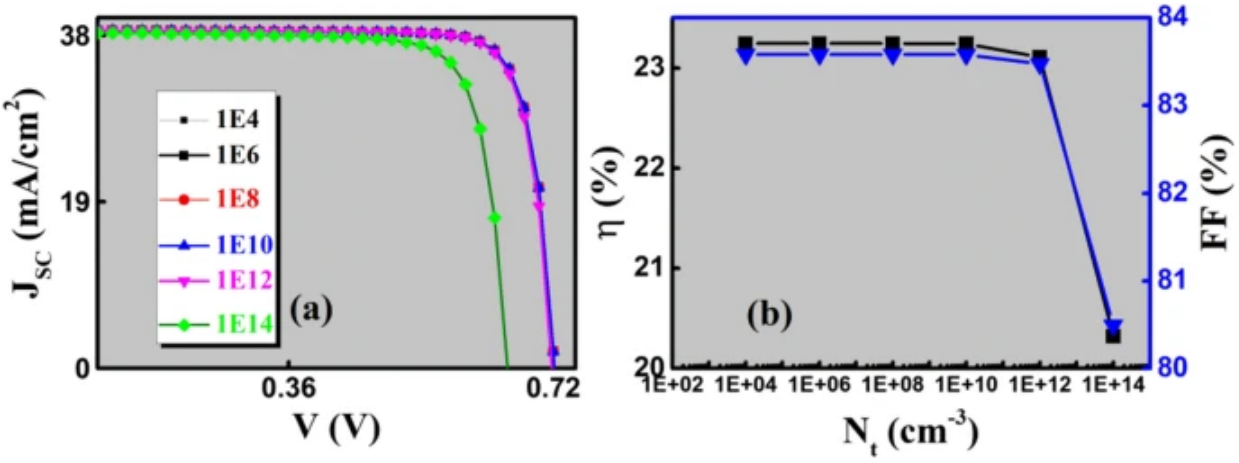

Influence of SnS absorber layer defect density on solar cell performance **a** J-V characteristics and **b** efficiency and Fill Factor

The relation of minority carrier lifetime (\(\tau\)) with the defect density and the carrier diffusion length (\({L}_{D}\)) with mobility parameter, respectively, is represented in Eqs. (1) and (2) as follows (Baig 2018; Niemeyer 2017; Hodes and Kamat 2015):

$${\tau }_{\left(n,p\right)}=\frac{1}{{\delta }_{(n,p)}{\nu }_{th}{N}_{t}}$$

(1)

$${L}_{{D}_{(n,p)}}=\sqrt{{\mu }_{(n,p)}\frac{kT}{q}{\tau }_{\left(n,p\right)}}$$

(2)

where \({\tau }_{\left(n,p\right)}\) is minority carrier lifetime, \({\delta }_{(n,p)}\) is the capture cross-section area for electron and hole, \({\nu }_{th}\) is the thermal velocity of carriers, N_t is defect density in the absorber layer, and the carrier diffusion length is dependent on the product of \({\mu }_{(n,p)}\) carrier mobility and minority carrier lifetime. For the SnS absorber layer, the values of τ and L_D decrease with increasing order of N_t as shown in Fig. 8.

Fig. 8

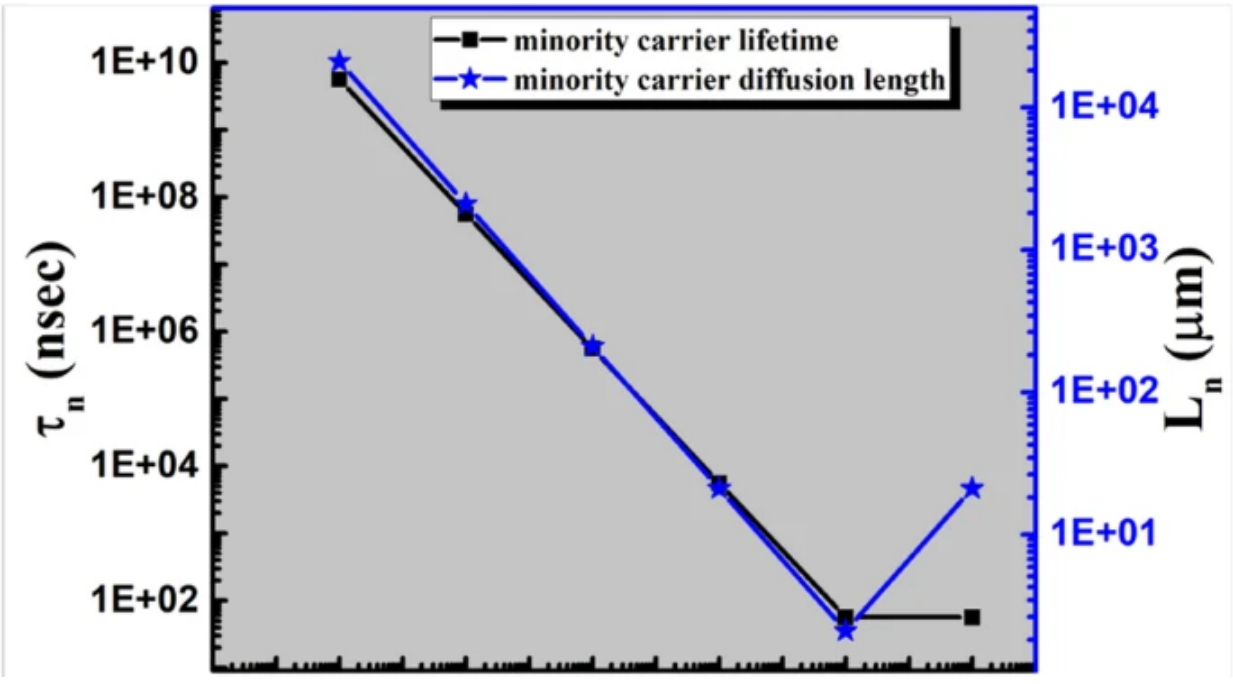

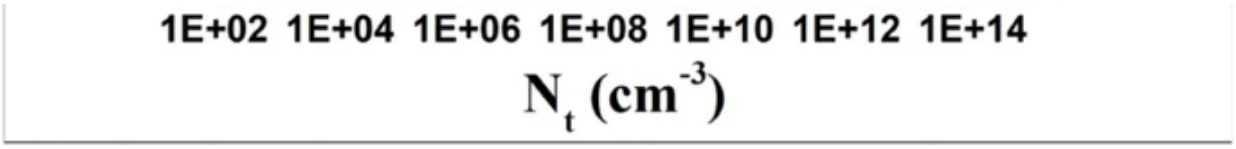

Minority carrier lifetime (τ_n) and diffusion length (L_n) vs defect density in p-SnS

Interface between SnS/CdS layers

As shown in Fig. 9a with the increase in defect density from $N_t = 5 \times 10^1$ cm^{-2} to $N_t = 5 \times 10^{11}$ cm^{-2} at the SnS/CdS interface, the solar cell performance remains constant until $N_t = 5 \times 10^7$ cm^{-2} and then decreases. Figure 9b shows, at the maximum defect density value $N_t = 5 \times 10^{11}$ cm^{-2}, the efficiency of solar cell decreases from $\eta = 23.24\%$ to $\eta = 20.32\%$. As the interface defects lead to the interface recombination such as Shockley–Read–Hall (SRH) recombinations and with the short carrier lifetime, the rate of recombination increases, hence attributed to degradation in the performance of the solar cell (Cho 2019, 2020).

Fig. 9

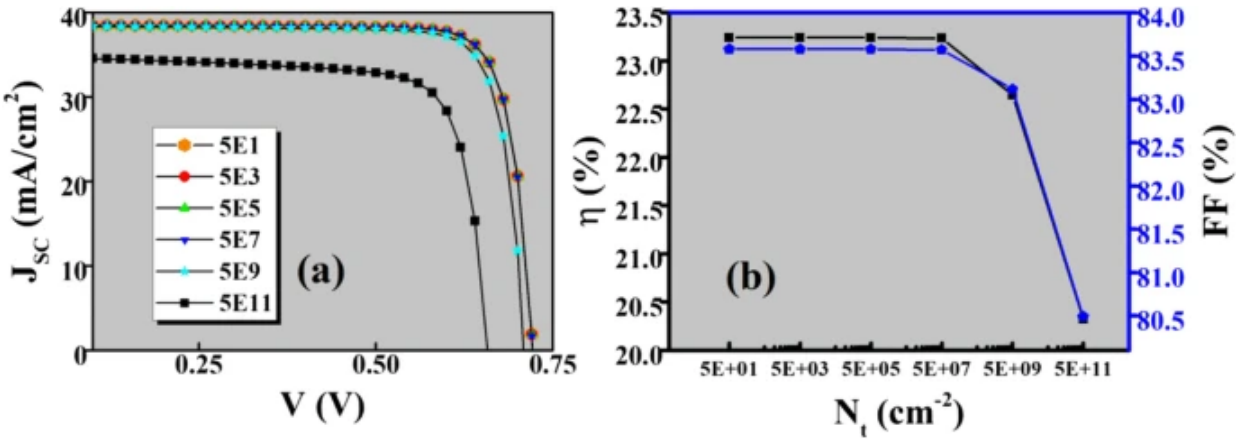

a J-V characteristics and **b** FF and efficiency of solar cell for interface defect density.

Impact of temperature

The PV parameters, both the V_{oc} and J_{sc}, are controlled by temperature-dependent factors such as bandgap, generation of electron–hole pairs, and saturation current (Singh 2008; Nguyen 2020). Thus, we performed an ambient temperature-dependent simulation using SCAPS-1D for SnS/CdS/ZnMgO TFSCs. The photovoltaic characteristics have been analyzed with various temperatures (in the range of

240 to 390 K) and keeping all other parameters constant. The simulated results are depicted in Fig. 10; we observed as the temperature increases higher than R.T. (300 K), the bandgap of the materials are affected which directly impact the band alignment of heterojunction and the generation of electron–hole pairs, further decreasing efficiency and FF with V_{oc} (Garain et al. 2021; Todorov 2017).

Fig. 10

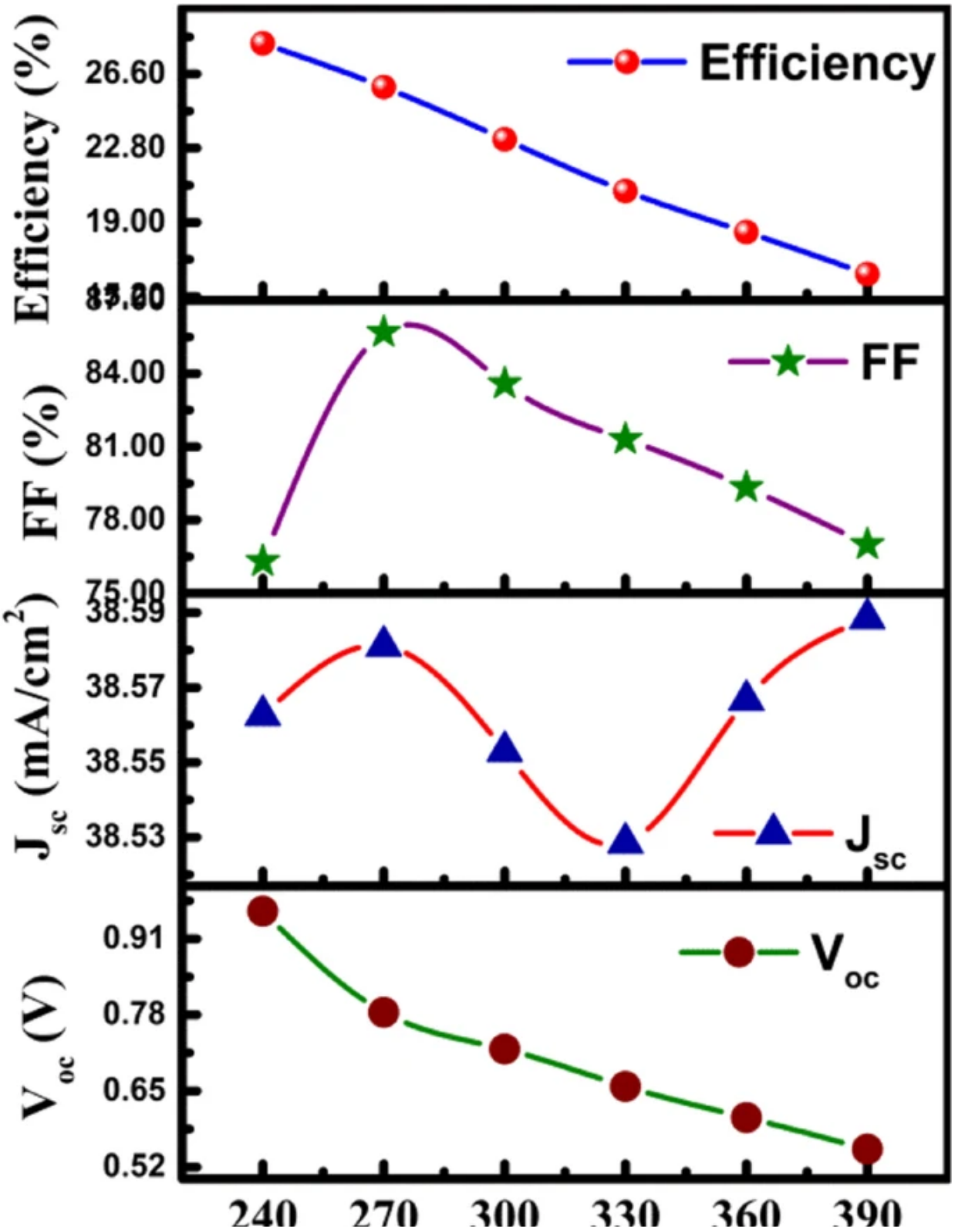

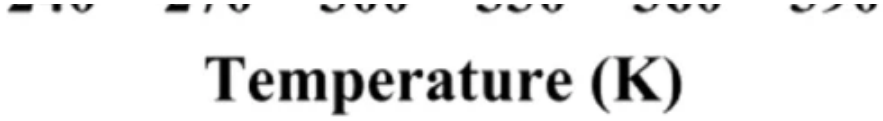

Temperature-dependent solar cell performance for SnS TFSCs

Conclusion

In this report, the p-SnS/n-ZnMgO cell structure has been modified by entering the CdS buffer layer to improve the performance and numerically simulated with the SCAPS-1D simulation program. In the performance enhancement of SnS TFSCs, parameters like thickness, defect density, thermal stability (temperature), and doping concentration are varied and their effects are analyzed. Initially, the band-alignment engineering was tuned by controlling the concentration of Mg in the ZnMgO window layer with buffer and absorber layers. The minimum CBO between SnS/CdS interface and CdS/ZnMgO interface help to improve the overall performance of the device. However, Mg concentration (x) = 0.18 shows the better results (Voc = ~ 0.7 V, short-circuit current density (Jsc) = 38.54 mA/cm^2, Fill Factor = 83%, and efficiency (η) = ~ 23%) with minimum band-offset at the CdS/ZnMgO interface, and the hexagonal nanorod-like morphology of ZnMgO helps to improve open-circuit voltage. However, CdS buffer layer with a minimum thickness (t = 50 nm) helps to reduce the effect of maximum defect density at SnS/CdS interface. As a result with $N_t = 1 \times 10^{11}$ cm^{-2} at SnS/CdS interface, the optimal Voc = 0.7 V and Jsc = 32 mA/cm^2 is higher compared to that of reported experimental values Voc = 0.230 V and Jsc = 12.1 mA/cm^2. In the end, with all optimized parameters, the proposed p-SnS/CdS/n-ZnMgO-modified cell structure optimal efficiency is 20% which is quite larger than the experimentally reported p-SnS/n-ZnMgO cell structure efficiency of 2.1%. It is concluded that this current investigation with the modified array and optimized parameters for SnS-based TFSCs promises the achievement of higher efficiency. From the experimental perspective, this design with optimal cost-performance seems logical and reliable, and could be feasible to implement.

References

Andrade-Arvizu JA, Courel-Piedrahita M, Vigil-Galán O (2015) SnS-based thin film solar cells: perspectives over the last 25 years. J Mater Sci: Mater Electron 26(7):4541–4556

CAS Google Scholar

Baig F et al (2018) Numerical analysis a guide to improve the efficiency of experimentally designed solar cell. Appl Phys A 124(7):471

Article Google Scholar

Bittau F et al (2018) Analysis and optimisation of the glass/TCO/MZO stack for thin film CdTe solar cells. Sol Energy Mater Sol Cells 187:15–22

Article CAS Google Scholar

Burgelman M et al (2007) Numerical simulation of thin film solar cells: practical exercises with SCAPS

Chantana J et al (2019) Characterization of Cd-free Zn1−xMgxO:Al/Zn1−xMgxO/Cu(In,Ga)(S,Se)2 solar cells fabricated by an all dry process using ultraviolet light excited time-resolved photoluminescence

Cho JY et al (2019) Controlled thickness of a chemical-bath-deposited CdS buffer layer for a SnS thin film solar cell with more than 3% efficiency. J Alloy Compd 796:160–166

Article CAS Google Scholar

Cho JY et al (2020) Achieving over 4% efficiency for SnS/CdS thin-film solar cells by improving the heterojunction interface quality. J Mater Chem 8(39):20658–20665

Article CAS Google Scholar

Devika M et al (2008) Ohmic contacts to SnS films: selection and estimation of thermal stability. J Appl Phys 104(12):124503

Article Google Scholar

Garain R, Basak A, Singh UP (2021) Study of thickness and temperature dependence on the performance of SnS based solar cell by SCAPS-1D. Mater Today 39:1833–1837

CAS Google Scholar

Gharibshahian I, Sharbati S, Orouji AA (2018) Potential efficiency improvement of Cu (In, Ga) Se2 thin-film solar cells by the window layer optimization. Thin Solid Films 655:95–104

Article CAS Google Scholar

Ghosh B et al (2011) Fabrication of CdS/SnS heterostructured device using successive ionic layer adsorption and reaction deposited SnS. Thin Solid Films 519(10):3368–3372

Article CAS Google Scholar

Haleem AMA, Ichimura M (2010) Experimental determination of band offsets at the SnS/CdS and SnS/InSxOy heterojunctions. J Appl Phys 107(3):034507

Article Google Scholar

Hertwig R et al. (2020) ALD-ZnMgO and absorber surface modifications to substitute CdS buffer layers in co-evaporated CIGSe solar cells. EPJ Photovolt 11

He X et al (2018) Simulation of high-efficiency CdTe solar cells with Zn1-x Mg x O window layer by SCAPS software. Mater Res Express 5(6):065907

Article Google Scholar

He X et al (2019) The Band Structures of Zn1-xMgxO(In) and the simulation of CdTe solar cells with a Zn1-xMgxO(In) window layer by SCAPS. Energies 12:291

Article CAS Google Scholar

Hodes G, Kamat PV (2015) Understanding the implication of carrier diffusion length in photovoltaic cells. J Phys Chem Lett 6(20):4090–4092

Article CAS Google Scholar

Klochko NP et al (2016) Development of a new thin film composition for SnS solar cell. Sol Energy 134:156–164

Article CAS Google Scholar

Maity S, Sahu PP (2019) Efficient Si-ZnO-ZnMgO heterojunction solar cell with alignment of grown hexagonal nanopillar. Thin Solid Films 674:107–111

Article CAS Google Scholar

Minbashi M et al (2018) Simulation of high efficiency SnS-based solar cells with SCAPS. Sol Energy 176:520–525

Article CAS Google Scholar

Mohammadnejad S, MollaaghaeiBahnamiri Z, EnayatiMaklavani S (2020) Enhancement of the performance of kesterite thin-film solar cells using dual absorber and ZnMgO buffer layers. Superlattice Microst 144:106587

Article CAS Google Scholar

Nguyen D (2020) Modelling and numerical analysis of ZnO/CuO/Cu2O heterojunction solar cell using SCAPS. Engineering Research Express 2

Niemegeers A, Burgelman M, Vos AD (1995) On the CdS/CuInSe2 conduction band discontinuity. Appl Phys Lett 67(6):843–845

Article CAS Google Scholar

Niemeyer M et al (2017) Minority carrier diffusion length, lifetime and mobility in p-type GaAs and GaInAs. J Appl Phys 122(11):115702

Article Google Scholar

Omrani MK et al (2018) Improve the performance of CZTSSe solar cells by applying a SnS BSF layer. Solid-State Electron 141:50–57

Article CAS Google Scholar

Rajpal S and SR Kumar (2019) Effect of Mg concentration on the structural, morphological and optical properties of ternary ZnMgO nanocrystalline thin films. in Innovation in materials science and engineering. Singapore: Springer Singapore

Ramakrishna Reddy KT, Koteswara Reddy N, Miles RW (2006) Photovoltaic properties of SnS based solar cells. Sol Energy Mater Sol Cells 90(18):3041–3046

Article CAS Google Scholar

Reddy KTR et al (2011) Studies on the energy band discontinuities in SnS/ZnMgO Thin film heterojunction.

Rühle S (2016) Tabulated values of the Shockley–Queisser limit for single junction solar cells. solar energy

Singh P et al (2008) Temperature dependence of I-V characteristics and performance parameters of silicon solar cell. Sol Energy Mater Sol Cells 92(12):1611–1616

Article CAS Google Scholar

Sinsermsuksakul P et al (2014) Overcoming efficiency limitations of SnS-based solar cells

Tebyetekerwa M et al (2019) Quantifying quasi-Fermi level splitting and mapping its heterogeneity in atomically thin transition metal dichalcogenides. Adv Mater 31(25):1900522

Article Google Scholar

Todorov TK et al (2017) Ultrathin high band gap solar cells with improved efficiencies from the world's oldest photovoltaic material. Nat Commun 8(1):682

Article Google Scholar

Xu J, Yang Y (2014) Study on the performances of SnS heterojunctions by numerical analysis. Energy Convers Manage 78:260–265

Article Google Scholar

Acknowledgements

This manuscript is part of the special issue of selected papers from the 6th edition of the biennial International Conference on Nanoscience and Nanotechnology (ICONN-2021). The authors would like to express their gratitude to Dr. Fouran Singh, Inter-University Accelerator Centre (IUAC), New Delhi, for the prolific discussion. The author also acknowledges Dr. Marc Burgelman from the University of Gent for providing SCAPS simulation software.

Funding

This study received funding from the Inter-University Accelerator Centre (IUAC), New Delhi, through project number IUAC/XIII.3A/62307 dated 11/08/2017.

Author information

Authors and Affiliations

Department of Physics, Dr. Babasaheb Ambedkar Marathwada University, Aurangabad, MS, 431004, India

Vishnu V. Kutwade, Makrand E. Sonawane & Ramphal Sharma

Department of Nanotechnology, Dr. Babasaheb Ambedkar Marathwada University, Aurangabad, MS,

431004, India

Ketan P. Gattu, Dipak A. Tonpe & Ramphal Sharma

Department of Physics, Dayanand Anglo-Vedic (PG) College, Kanpur, India

Manoj K. Mishra

Corresponding author

Correspondence to Ramphal Sharma.

Ethics declarations

Conflict of interest

The authors declare no competing interests.

Additional information

Publisher's note

Springer Nature remains neutral with regard to jurisdictional claims in published maps and institutional affiliations.

Rights and permissions

Reprints and permissions

About this article

Cite this article

Kutwade, V.V., Gattu, K.P., Sonawane, M.E. *et al.* Contribution in PCE enhancement: numerical designing and optimization of SnS thin film solar cell. *J Nanopart Res* **23**, 146 (2021). https://doi.org/10.1007/s11051-021-05259-5

Received	Accepted	Published
12 January 2021	06 June 2021	12 July 2021

DOI
https://doi.org/10.1007/s11051-021-05259-5

Share this article

Anyone you share the following link with will be able to read this content:

Get shareable link

Provided by the Springer Nature SharedIt content-sharing initiative

Keywords

SnS simulation SCAPS-1D PCE Band alignment QE

Solar energy conversion